Available online at www.sciencedirect.com
ScienceDirect
International Journal of Heat and Fluid Flow 27 (2006) 945–954
International Journal of HEAT AND FLUID FLOW
www.elsevier.com/locate/ijhff

Dynamic self-organization in particle-laden channel flow

Bernard J. Geurts [a,b,*], Bert Vreman [c]

[a] Multiscale Modeling and Simulation, Department of Applied Mathematics, University of Twente, P.O. Box 217, 7500 AE Enschede, The Netherlands
[b] Anisotropic Turbulence, Fluid Dynamics Laboratory, Eindhoven University of Technology, P.O. Box 513, 5300 MB Eindhoven, The Netherlands
[c] Vreman Research, Godfried Bomansstraat 46, 7552 NT Hengelo, The Netherlands

Received 23 September 2005; received in revised form 7 February 2006; accepted 4 March 2006
Available online 27 June 2006

Abstract

We study dynamic flow-structuring and mean-flow properties of turbulent particle-laden riser-flow at significant particle volume fractions of about 1.5%. We include particle–particle as well as particle–fluid interactions through inelastic collisions and drag forces, in a so-called four-way coupled description. These interactions are the origin for the emergence of coherent particle swarms in a flow. The dynamic cluster-formation and cluster-disintegration are associated with the competition between turbulent dispersion and inelastic particle collisions. We establish the basic scenario of this self-organization and investigate the dominant mean-flow aspects of the resulting turbulence modulation for particles with high Stokes response-time. Large-eddy simulations of turbulent channel flow, using dynamic subgrid models and particles at a significant volume fraction and realistic mass load are presented. These simulations indicate the development of a thinner boundary layer, a flatter velocity profile, an higher effective Von Kármán constant and an accumulation of particles near the walls. Moreover, it was found that neglecting particle–particle interactions, as done in so-called two-way coupling, leads to a modulated flow which displays a strong 'center-channel-jet' that is not found in physical experiments.
© 2006 Elsevier Inc. All rights reserved.

PACS: 02.60.Cb; 47.27.Eq; 47.55.Kf

Keywords: Turbulence; Particle-laden flow; Large-eddy simulation; Channel flow; Inelastic collisions; Coherent structures; Four-way coupling; Turbulence modulation

1. Introduction

Many flows of relevance to large-scale chemical processing involve solid catalyst particles at significant concentrations, embedded in a carrying gas-flow. Control over the spatial distribution of the catalyst particles, especially its homogeneity, is essential in order to provide a chemical processing that is as complete and uniform as possible, that is consistent with modern environmental requirements and that does not constitute a strong safety hazard. This provides the main application context for this study which is directed toward understanding the flow-structuring and statistical aspects of turbulent gas-solids flow in a vertical channel. Specifically, we concentrate on the development of a large-eddy simulation strategy with which the central up-scaling of laboratory-scale experiments to realistic industrial settings can be supported.

The control of large-scale chemical processes is hindered by the lack of precise prediction-tools which characterize the dynamics in systems of realistic proportions. Since full-scale experimental research is costly and often not precise or not feasible, the development of accurate simulation tools is very important. A specific example is the cracking of oil which is facilitated by adding large numbers of catalyst particles to a carrying gas-flow. Basic to catalyst cracking is an understanding of the granular dynamics of large swarms of grains of sand. Specifically, it is important to

* Corresponding author. Address: Multiscale Modeling and Simulation, Department of Applied Mathematics, University of Twente, P.O. Box 217, 7500 AE Enschede, The Netherlands.
E-mail address: b.j.geurts@utwente.nl (B.J. Geurts).

0142-727X/$ - see front matter © 2006 Elsevier Inc. All rights reserved.
doi:10.1016/j.ijheatfluidflow.2006.03.025

investigate whether particle–particle collisions are dynamically important and lead to large clusters, thus contributing to spatial non-uniformities that may jeopardize safety and product-consistency and increase pollution.

The particles interact among each other mainly through inelastic collisions which by themselves lead to a granular clustering. In Fig. 1 an illustration of the clustering in a granular medium is provided (Lohse et al., 2004) which may be loosely associated with the clustering behavior seen in large ensembles of catalyst particles in a riser flow. The dynamic occupation of part of the flow-domain by quite dense regions of particles induces an important alteration of the overall flow, compared to the clean channel flow.

The dynamical behavior of the embedded particle-ensemble is quite complex and interacts nonlinearly with the carrying gas-flow (Elghobashi and Truesdell, 1993). The particles are dragged along by the gas-flow, exchanging momentum with it through a friction force-density. This arises since the particles cannot instantaneously respond to the gas-flow. Instead, a so-called Stokes response-time (Maxey and Riley, 1983; Bagchi and Balachandar, 2003) is introduced to represent the degree of 'sluggishness' with which the particles follow changes in the gas-flow. Moreover, the discrete particles interact among each other, e.g., through inelastic particle–particle collisions. In case only particle–fluid interactions are incorporated the description is referred to as 'two-way coupled' while a 'four-way coupled' formulation arises when also the particle–particle interactions are included, e.g., (Elghobashi and Truesdell, 1993; Hoomans et al., 1996). At sufficiently low particle volume fraction the two-way coupling will be adequate. However, with increasing particle volume fraction the collisions will become dynamically significant and the more involved four-way coupling will be required.

The main purpose of this paper is to demonstrate in the context of numerical simulation that for rather coarse particles, at a realistic mass load around 20 and a modest particle volume fraction of about 1.5%, the collisions constitute a major dynamic effect that needs to be incorporated in order to retain a physically reliable flow description. This forms a separate confirmation of the commonly accepted classification in which volume fractions larger than 10^{-3} necessitate the inclusion of particle–particle collisions (Elghobashi and Truesdell, 1993).

The present study is among the first to establish the relevance of the particle–particle collisions, at moderately high volume fractions, using detailed turbulence simulations. Without the four-way coupling, the continual process of dynamic self-organization of the embedded particles in coherent swarms and the subsequent destruction of such 'clusters', is completely missed in the computational model. In fact, the computationally more appealing two-way coupling model appears to give rise to predictions that are qualitatively unreliable at sufficiently high volume fractions. As an example, instead of the experimentally observed flattening of the velocity profile in the gas-phase (Tsuji et al., 1984) compared to the clean channel flow, the two-way coupling model gives rise to an unexpected rather strong 'center-channel-jet'. These and other shortcomings of the two-way coupling model will be further clarified in this paper.

The two-phase gas-solids flow is governed by an interplay between the nonlinearity of the convective fluxes and the particle–fluid and particle–particle interactions. These

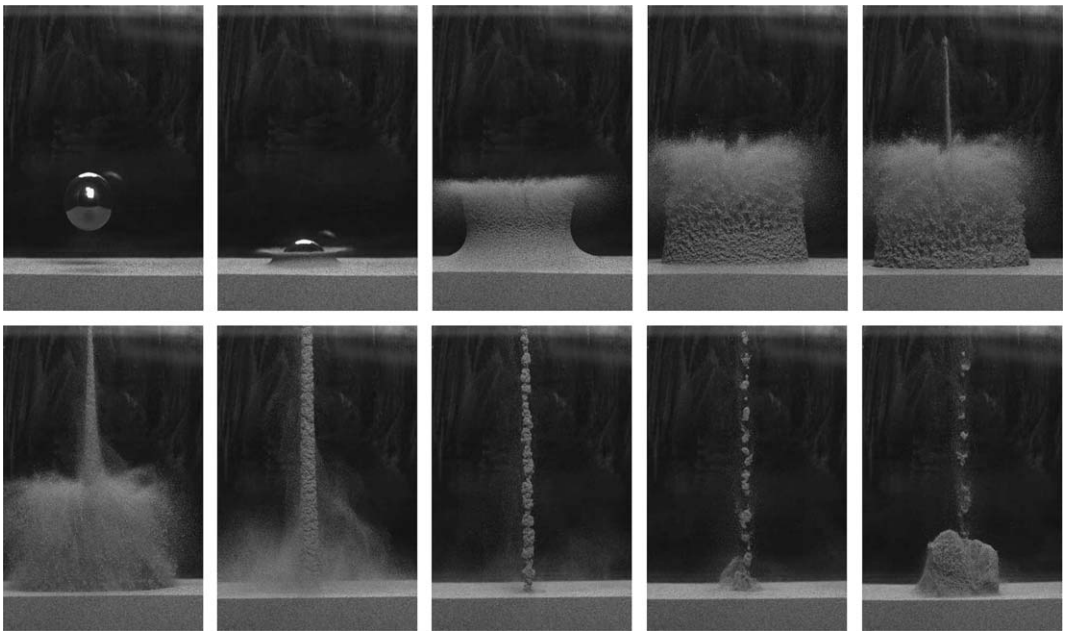

Fig. 1. A sand-jet arising after the impact of a heavy sphere in a loose sand-bed. A primary eruption follows from the initial impact after which a sand-jet is formed. As this column of sand starts to fall down, inelastic collisions among the sand-particles give rise to the formation of granular clusters. Further details: http://pof.tnw.utwente.nl/3_research/3_gallery.htm/.

effects may accumulate and significantly modify basic turbulence properties. As an example, large-scale dynamic flow-structuring may arise which affects the flow-statistics compared to the case with no or only weak particle contributions. These flow-alterations constitute the so-called 'modulation of turbulence' which, e.g., seriously complicates the prediction of the up-scaling of flow-phenomena from laboratory-scale experiments to industrial-scale settings. The case of small bubbles embedded in a flow of water was recently investigated experimentally in (Rensen et al., 2005), a slight steepening of the kinetic energy spectrum was reported as a result of the bubbles. In this paper we consider the gas-solids system and quantify the turbulence-modulation via changes in the mean-flow properties.

In this paper, we adopt the large-eddy simulation approach and extend some of our earlier work on this topic as reported in (Vreman et al., 2004). In the present paper we consider the formation of coherent particle structures in more detail and compute mean-flow properties of the gas and solids phase. Other computational studies found in literature involve considerably lower particle volume fractions, typically 10^{-4} or lower (Yamamoto et al., 2001; Squires and Simonin, 2002; Marchioli et al., 2003). In these studies particle collisions and even particle–fluid interactions are often not taken into account. In contrast, in this paper we study dynamic consequences of both particle–particle as well as particle–fluid interactions at relatively high volume fractions. We incorporate two dynamic subgrid models in order to assess the sensitivity of the predictions. The standard eddy-viscosity model (Germano et al., 1991) and a faster but approximate version based on Taylor expansions (Vreman et al., 2004) are incorporated.

Before going into detail, the main findings may be summarized as follows. Incorporating particle–fluid and particle–wall interactions induces a thinning of the boundary layer, leading to an higher skin-friction coefficient. Moreover, the additional inelastic collisions considered in the four-way description give rise to a flatter velocity profile, corresponding to an higher Von Kármán constant, and cause a striking dynamic self-organization. A clustering tendency associated with the inelastic collisions competes with the strong turbulent dispersion in the channel flow. Starting from a dispersed particle distribution, in the course of time larger clusters may be formed due to inelastic collisions. These collisions represent a spatially distributed loss of energy which effectively contributes to the viscous dissipation. As the clusters develop, the turbulence intensities in the adjacent 'clean' regions grow, unhindered by the mentioned extra dissipation associated with the collisions. Subsequently, this may lead to a 'bursting' of the clusters that formed, etc. The clusters display large variations in size and shape and represent the degree of spatial non-uniformity that may be induced under suitable flow-conditions in gas-solids flows. The clustering process occurs only in the four-way coupled description.

The organization of this paper is as follows. In Section 2, we present the mathematical model and provide the large-eddy formulation of the particle-laden flow. Subsequently, the dynamic flow-structuring is sketched in Section 3. The corresponding turbulence modulation is discussed quantitatively in Section 4. Finally, some concluding remarks are collected in Section 5.

2. Large-eddy formulation of particle-laden flow

The computational model distinguishes a gas-phase and a solids-phase which will be specified in this section. The embedded solids particles are considered to be small compared to convective turbulent length-scales. This allows to effectively approximate the equations for the gas-phase in terms of flow through a (time- and position-dependent) porous medium (Whitaker, 1996). The treatment of the solids phase follows a deterministic model as specified in (Hoomans et al., 1996). Finally, we will describe the large-eddy treatment of the gas-phase.

Gas-phase. We first turn to the particle-laden gas-phase. We consider small spherical particles with radius a and volume $V_\mathrm{p} = 4\pi a^3/3$. The porosity $\varepsilon_V(\mathbf{x},t)$ associated with a small volume $V \gg V_\mathrm{p}$ around the point $\mathbf{x}$ at time t can be defined as:

$$\varepsilon_V(\mathbf{x},t) = 1 - \frac{n_V(\mathbf{x},t)V_\mathrm{p}}{V} \tag{1}$$

where $n_V(\mathbf{x},t)$ is the number of particles in V at time t. In terms of ε_V we observe that $\varepsilon_V \to 1$ in case V does not contain any particles while $\varepsilon_V \to 0$ if the volume V contains no gas. In the continuum-limit, the porosity is denoted by ε. The Navier–Stokes equations that govern the flow in a porous medium specified by ε read:

$$\begin{aligned}
&\partial_t(\rho\varepsilon) + \partial_j(\rho\varepsilon u_j) = 0\\
&\partial_t(\rho\varepsilon u_i) + \partial_j(\rho\varepsilon u_i u_j) = -\partial_i(\varepsilon p) + \partial_j(\varepsilon\sigma_{ij})\\
&\qquad\qquad + (\rho\varepsilon g - \partial_i(\varepsilon P_m))\delta_{i3} + f_i\\
&\partial_t(\varepsilon e) + \partial_j((e+p)\varepsilon u_j) = \partial_j(\varepsilon\sigma_{ij}u_i) + (\rho\varepsilon g - \partial_3(\varepsilon P_m))u_3\\
&\qquad\qquad + f_i u_i - \partial_j(\varepsilon q_j)
\end{aligned} \tag{2}$$

where the symbols ∂_t and ∂_j denote the partial differential operators $\partial/\partial t$ and $\partial/\partial x_j$ respectively. Furthermore, ρ is the density, $\mathbf{u}$ the velocity, p the pressure and $e = p/(\gamma-1) + \rho\, u_k u_k/2$ the total energy per unit volume. The constant γ denotes the fraction of specific heats $\gamma = C_\mathrm{P}/C_V = 1.4$. The flow is driven by a pressure gradient in the vertical direction, involving the imposed mean pressure P_m which is assumed a function of time and x_3 only, such that the total fluid mass flow is kept constant.

In the system of Eq. (2) we selected the conservative formulation following, e.g., Whitaker (1996) and Lakehal et al. (2002). This facilitates the use of the conservative finite volume method in the simulations. The conservative formulation gives rise to pressure gradient contributions that incorporate the porosity ε inside the spatial derivative operators. Alternative formulations may be found in

literature in which, e.g., $\varepsilon\partial_i p$ arises instead (Zhang and Prosperetti, 1997). The latter formulation is formally equivalent to the one selected here, provided a corresponding adaptation in the interpretation of the force terms f_i is included. The distinction between these formulations can be traced back to differences in the interpretation of the (volume averaged) gas-velocity as explained in (Whitaker, 1996) and adopted by (Breugem and Boersma, 2005; Breugem and Rees, 2006). In the formulation of Zhang and Prosperetti (1997), the force-terms f_i include the drag force arising from the relative motion of the particles and the fluid. In the conservative formulation as adopted in this paper, the terms $(p + P_m)\partial_i\varepsilon$ are incorporated in f_i as well, to restore the formal equivalence with (Zhang and Prosperetti, 1997). This extended definition of f_i for the conservative formulation is also required in order to keep the equations physically consistent for the special case of non-uniform porosity ε and neutrally buoyant particles. In fact, if there is no fluid motion and the embedded particles have the same density as the fluid then no large-scale motion should spontaneously develop from gradients in the porosity ε. However, the pressure-related contributions in the conservative formulation would imply a non-zero contribution $(p + P_m)\partial_i\varepsilon$ which needs to be compensated by the corresponding extension of the forces f_i. In strongly turbulent flow and at the modest particle concentrations considered in this paper, the additional contributions $(p + P_m)\partial_i\varepsilon$ were found to be of little dynamical importance. In particular, the statistical properties of the fluid – and particle-phase as predicted by the conservative formulation using the complete definition of f_i or with the drag force alone, were observed to be quite identical.

The viscous stress tensor σ_{ij} is defined as the product of viscosity $\mu = 3.47 \times 10^{-5}$ kg/(m s) and strain-rate tensor $S_{ij} = \partial_i u_j + \partial_j u_i - \frac{2}{3}\delta_{ij}\partial_k u_k$. The heat-flux q_j is defined as $-\kappa\partial_j T$ where T is the temperature and $\kappa = 0.035$ W/(mK) the heat-conductivity coefficient. Pressure, density and temperature are related to each other by the equation of state for an ideal gas $\rho RT = M_{\text{gas}}p$ where $R = 8.314$ J/(mol K) is the universal gas constant and $M_{\text{gas}} = 0.0288$ kg/mol is the mass of the gas per mole. The gravitational acceleration in the momentum equation equals $g = -9.81$ m/s^2 and f_i denotes the force of the particles on the flow per volume unit. These are induced by an effective relative motion of the particles with respect to the gas which gives rise to drag forces on the fluid (Hoomans et al., 1996). To obtain f_i the drag force due to each particle is distributed over the eight nearest neighboring grid-points of the computational cell in which the particle is found. For the distribution of these forces a weighted average is used which takes the distances between these grid points and the actual particle location into account (Hoomans et al., 1996).

The coordinate x_3 denotes the streamwise, x_2 the normal and x_1 the spanwise direction. The domain is rectangular and the channel width, height and depth equal $L_2 = 0.05$ m, $L_3 = 0.30$ m and $L_1 = 0.075$ m, respectively. No-slip boundary conditions are imposed in the x_2-direction and periodic boundary conditions are assumed for the stream- and spanwise directions.

The equations formulated in (2) are equivalent to the equations governing a compressible ideal gas with velocity $\mathbf{u}$, temperature T, density $\hat{\rho} = \varepsilon\rho$, pressure $\hat{p} = \varepsilon p$, viscosity $\hat{\mu} = \varepsilon\mu$ and heat-conductivity $\hat{\kappa} = \varepsilon\kappa$. Therefore, to solve this flow it is convenient to use a compressible flow solver with additional forcing terms representing gravity and the forces from the particles on the fluid. For a channel flow without particles the pressure gradient corresponds to wall shear-stress $\tau_w = 0.0625$ N/m^2, shear velocity $u_\tau = 0.25$ m/s and corresponding Reynolds number $Re_\tau = 180$. We will simulate a section of a riser flow with a vertical velocity of about 4 m/s. The parameters of the gas in the riser are close to those for air. The initial gas density equals $\rho_1 = 1.0$ kg/m^3 and we use a Mach number of ≈ 0.2 for which the turbulence is effectively incompressible.

The inclusion of compressibility effects as shown in (2), appears not strictly necessary for the volume fractions considered here. The primary flow-physics associated with an average volume fraction of 1.5% as studied in this paper, can probably also be captured using an incompressible flow model. However, the fluctuations in the particle density were found to occassionally give rise to higher local volume fractions of up to 10% for which compressible corrections are sensible. So, although the fluid-particle and particle–particle energy interactions are considered dynamically not important in the modeling adopted here, the compressible flow model is used as it is more complete, without distracting from our main focus nor adding to the computational costs.

Solids-phase. The discrete particle model calculates the motion of particles in the fluid and includes inelastic particle collisions. The mean velocity of the riser is low enough to neglect the heat transfer during particle collisions. The particle diameter equals $d_p = 0.4$ mm and the particle density is $\rho_p = 1500$ kg/m^3. The number of particles equals $N_p = 419{,}904$. With these parameters the average volume fraction is 0.013 and the Stokes response-time is $\tau_p = (\rho_p d_p^2)/(18\mu) = 0.4$ s.

The motion of every individual particle i in the system is calculated from Newton's second law:

$$m_i \frac{\mathrm{d}\mathbf{v}_i}{\mathrm{d}t} = \frac{V_i\beta}{1-\varepsilon}(\mathbf{u} - \mathbf{v}_i) + m_i g\mathbf{e}_z + \mathbf{f}_i^{pp} + \mathbf{f}_i^{pw}, \tag{3}$$

where m_i denotes the mass, $\mathbf{v}_i$ the velocity, V_i the volume of the ith particle and $\mathbf{e}_z$ denotes the vertical z-direction. The gravitational acceleration acts in the negative z-direction. The forces on the right hand side of the equation represent standard drag, gravity, particle–particle interaction ($\mathbf{f}_i^{pp}$) and particle–wall interaction ($\mathbf{f}_i^{pw}$), respectively. The general equation of motion for a single particle derived in (Maxey and Riley, 1983) contains additional forces, such as added mass and history terms. However, the recent comparison with DNS results reported in Bagchi and Balachandar (2003) did not show improvements when these forces were included.

The symbol β in the drag term is the inter-phase momentum transfer coefficient. For dense regimes it is frequently modeled through the Ergun equation ($\varepsilon < 0.8$):

$$\frac{\beta d_p^2}{\mu} = 150\frac{(1-\varepsilon)^2}{\varepsilon} + 1.75(1-\varepsilon)Re \tag{4}$$

whereas in the more dilute regime ($\varepsilon > 0.8$)

$$\frac{\beta d_p^2}{\mu} = \frac{3}{4}C_D Re(1-\varepsilon)\varepsilon^{-2.65};$$
$$C_D = \begin{cases} 24(1+0.15Re^{0.687})/Re; & Re < 10^3 \\ 0.44 & Re > 10^3 \end{cases} \tag{5}$$

Here $Re = \varepsilon\rho|\mathbf{u}-\mathbf{v}|a/\mu$ is the particle Reynolds number, which is evaluated at the particle position.

The collisions between the particles and between the particles and the solid channel walls are inelastic. These are described by a hard-sphere model in which it is assumed that the interaction forces are impulsive and therefore all other finite forces are negligible during collision. As a result of collisions, some of the kinetic energy is lost. This is described in terms of so-called 'restitution coefficients' which we take identical to (Hoomans et al., 1996).

Numerical method. The numerical method applies a second-order finite volume method for the spatial discretization. Moreover, a second order explicit Runge–Kutta time-stepping method with time-step 2×10^{-5} s for the fluid phase and Euler forward time-stepping with time step 10^{-4} s for the solids phase are adopted. Most of the computational effort is associated with the particle phase. The computational grid contains $32\times64\times64$ cells. The grid is non-uniform in the wall-normal direction with the first grid point at $y^+ \approx 1.5$. The porosity ε is determined on a uniform 'auxiliary' grid which is coarser than the particle diameter. Linear interpolation is used to communicate information between grid-nodes and particle positions.

The simulations run until at least $t = 5$ s, while statistics are accumulated between $t = 3$ s and $t = 5$ s. With a Stokes response-time of $\tau_p = 0.4$ s, the particles are evolved for $12.5\tau_p$ and the accumulation of the statistics is over $5\tau_p$. The particles considered in our simulation are highly inertial and in order to obtain quantitatively precise statistics, the averaging should preferably be over a more extended period. Averaging over shorter time-intervals will give rise to some statistical errors which may express themselves, e.g., as asymmetries in the average profiles of gas and solids properties such as velocity and turbulence intensities. Conversely, these asymmetries provide a first indication of the statistical averaging error. In the case studied in this paper we observed quite low levels of asymmetry already after averaging over only $5\tau_p$ (this may be inferred from the profiles presented in Section 4). Correspondingly, the main features of the average profiles and the influence of the solids-phase on these properties can be clearly discerned, despite the remaining statistical error. As the averaging process is known to converge quite slowly as function of the length of the averaging interval, it would be quite impractical to simulate for long enough for the statistical error to become virtually negligible. However, for the purpose of assessing and discerning the effects of two- and four-way coupled discrete particles, the adopted averaging interval appears well justified.

Large-eddy formulation. In order to make large-scale turbulent flow simulations at high particle volume fractions feasible, the gas-phase is described using large-eddy simulation (LES) (Geurts, 2003). The LES formulation is obtained by applying spatial filtering to the flow equations in order to reduce their dynamical complexity. In particular, we may consider convolution filtering in which

$$\overline{u} = L(u) = \int G(x-\xi)u(\xi)\,\mathrm{d}\xi = G * u \tag{6}$$

where $\overline{u}$ denotes the filtered solution and G the filter-kernel. The filter is assumed to be normalized, i.e., $L(1) = 1$. If the spatial filtering is applied to the governing equations the result may be expressed in terms of the LES-template: $\mathrm{NS}(\overline{U}) = R(U,\overline{U})$ where the original and filtered state-vector are defined by $U = [\varepsilon\rho, u_j, \varepsilon\mathrm{p}]$; $\overline{U} = [\overline{\varepsilon\rho}, \widetilde{u}_j, \overline{\varepsilon p}]$ with Favre-filtered velocity $\widetilde{u}_i = \overline{\rho\varepsilon u_j}/\overline{\rho\varepsilon}$. The spatial filtering yields a 'closure-residual' $R(U,\overline{U})$ which contains, e.g., the filtered forcing term $\overline{f}_i$ and the divergence of the turbulent stress tensor

$$\tau_{ij} = \overline{\rho\varepsilon u_i u_j} - \overline{\rho\varepsilon u}_i\overline{\rho\varepsilon u}_j/\overline{\rho\varepsilon} = \overline{\rho\varepsilon}\{\widetilde{u_i u_j} - \widetilde{u}_i\widetilde{u}_j\} \tag{7}$$

We restrict attention to explicit modeling of the turbulent stress tensor and evaluate other closure terms by calculating the original formulation in terms of the filtered variables. For the representation of the sub-filter scales we will next introduce two subgrid modeling approaches.

We incorporate dynamic subgrid modeling and begin with the standard eddy-viscosity assumption in the basic model, expressed by

$$m_{ij} = -\big[C_d\overline{\rho\varepsilon}\Delta^2 S(\widetilde{u})\big]S_{ij}(\widetilde{u}); \quad \Delta = (\Delta_1\Delta_2\Delta_3)^{\frac{1}{3}} \tag{8}$$

where Δ_i denotes the filter-width in the x_i-direction. The dynamic procedure (Germano et al., 1991) is based on the well-known Germano-identity and provides the possibility to calculate a 'Germano-optimal' coefficient C_d which adapts itself to the evolving flow. In fact, after some calculation and the usual approximations the dynamic coefficient C_d may be obtained from

$$C_d = \langle M_{ij}L_{ij}\rangle/\langle M_{ij}M_{ij}\rangle \tag{9}$$

with appropriately defined tensors L_{ij} for the resolved turbulent stress tensor and a tensor M_{ij} which collects subgrid model contributions on the filter-level ($\overline{\cdot}$) and the so-called test-filter level ($\widehat{\cdot}$). Here, $\langle\cdot\rangle$ represents an averaging over homogeneous directions and 'clipping' is applied in case the right-hand side of (9) would return negative values. We distinguish two implementations of the dynamic procedure, referred to as the 'standard' and the 'approximated fast' procedure. These may be defined as follows:

- *Standard dynamic procedure:* This requires explicit test-filtering and involves

$$L_{ij} = \widehat{[\overline{\rho\varepsilon}\widetilde{u}_i\widetilde{u}_j]} - \widehat{\overline{\rho\varepsilon}\widetilde{u}_i}\,\widehat{\overline{\rho\varepsilon}\widetilde{u}_j}/\widehat{\overline{\rho\varepsilon}} \tag{10}$$

$$M_{ij} = -\widehat{\overline{\rho\varepsilon}}(\sqrt{5}\Delta)^2 S(\widehat{\overline{\rho\varepsilon}\widetilde{u}}/\widehat{\overline{\rho\varepsilon}})S_{ij}(\widehat{\overline{\rho\varepsilon}\widetilde{u}}/\widehat{\overline{\rho\varepsilon}}) + \widehat{[\overline{\rho\varepsilon}\Delta^2 S(\widetilde{u})S_{ij}(\widetilde{u})]} \tag{11}$$

  where $\widehat{[\ldots]}$ denotes explicit application of the test-filter to the term between brackets.
- *Approximated fast procedure* (see Vreman, 2004, and its references): For common second order filters as adopted here we have $\widehat{w} = \overline{w} + \mathrm{O}(\Delta^2)$. Hence

$$L_{ij} \approx \frac{1}{3}\overline{\rho\varepsilon}\Delta_k^2\partial_k\widetilde{u}_i\partial_k\widetilde{u}_j; \quad M_{ij} \approx -4\overline{\rho\varepsilon}\Delta^2 S(\widetilde{u})S_{ij}(\widetilde{u}) \tag{12}$$

  This procedure is based on Taylor expansions and does not require explicit test-filtering which makes it computationally much cheaper.

In the next section, we will consider the dynamic self-organization that arises due to the 'competition' between the structuring associated with the inelastic particle collisions and the bursting of particle-clusters due to the underlying tendency of the clean flow to develop strong turbulence.

3. Dynamic particle-laden flow structuring at high concentration

In this section, we will show that the four-way coupling model gives rise to large-scale coherent particle swarms which are completely absent when the two-way coupling model is used.

In order to characterize the flow-structuring we concentrate on visualizing the particle volume fraction. For this purpose we introduce a uniform rectangular grid which contains $n_1 \times n_2 \times n_3$ cells respectively. The volume of each cell is denoted by V_{cell}. At time t we may count n particles in cell (i,j,k) and the corresponding volume fraction is $\psi = 1 - \epsilon_{\mathrm{cell}} = nV_{\mathrm{p}}/V_{\mathrm{cell}}$ where $V_{\mathrm{cell}} \gg V_{\mathrm{p}}$.

As point of reference, the basic riser flow was simulated using LES with the standard dynamic model and four-way coupling. The grid on which ψ is evaluated contains $32 \times 25 \times 64$ cells. We show the particle volume fraction at different times in Fig. 2. From these snapshots one may infer qualitatively the continual formation and

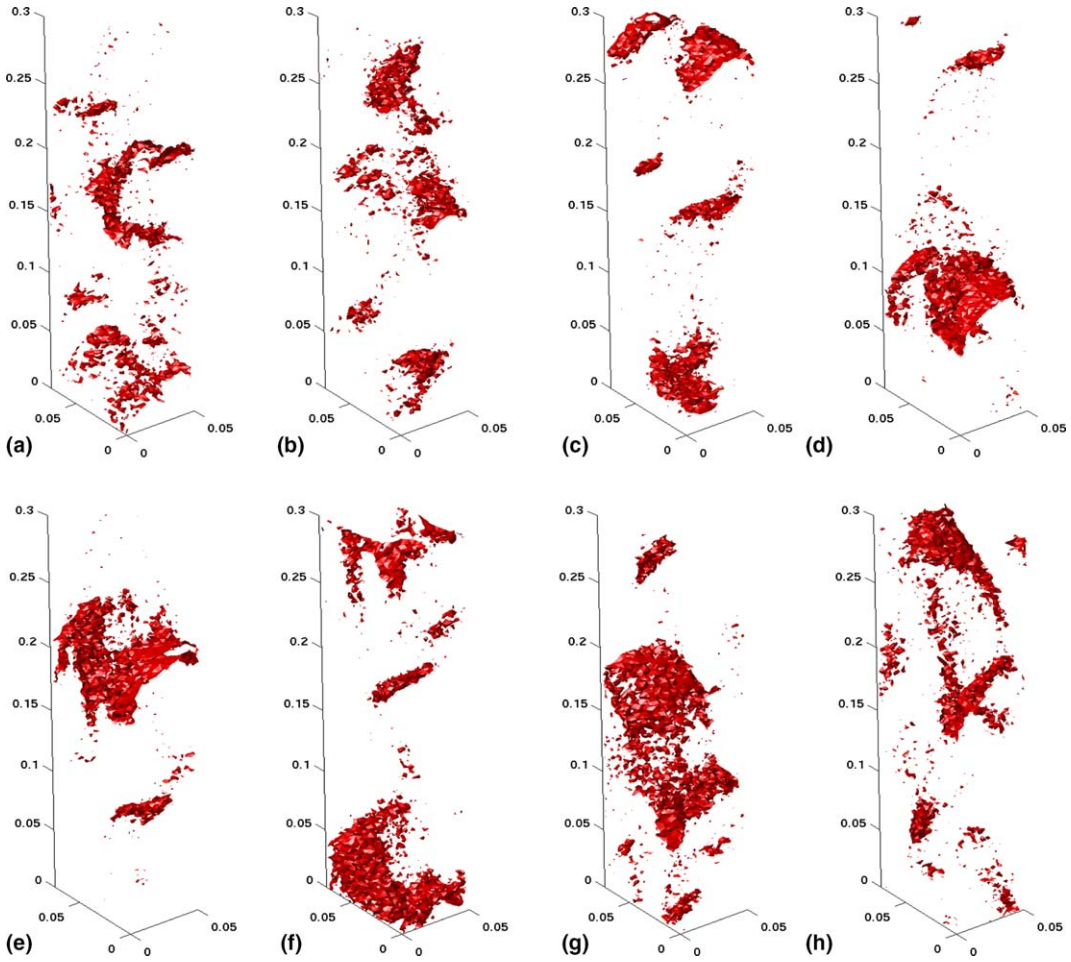

Fig. 2. Snapshots of the particle volume fraction showing iso-surfaces at $\psi = 0.03$ at $t = 3.1$ s (a) with steps of 0.05 until $t = 3.45$ s (h).

destruction of large-scale coherent structures in a self-contained manner which will be described next.

We start to describe the particle clustering and dispersion at an instant where ψ displays a rather fragmented distribution. In this state, the inelastic particle–particle collisions induce a spatially distributed loss of energy from the flow. After collision particles will generally separate more slowly than they moved toward each other before collision. At sufficiently high volume fraction such collisions occur at a rather high frequency and two nearby particles that just collided, may be hit by a third, only a short time later. After a few such *inelastic* collisions a small group of particles may form. This group can be hit by new particles and as a result these new particles will adapt their velocity toward the instantaneous average of the group. Hence, such 'fuzzy' groups can form the nucleation-core of a larger 'cluster', i.e., a region of higher particle density compared to the average density in the bulk. In Fig. 2 a more 'organized' state may be seen in Fig. 2(d–f) for example. Interaction with the turbulent gas-phase flow may subsequently disperse such clusters which leads to a new fragmented state from which a new sequence of clustering events may emerge. Clusters which happen to have grown quite large may also encounter larger, more energetic eddies in the flow which can split and disperse them in turn. In total a complex dynamical process arises with strong variability in the flow-structures that emerge. The self-organization seen in Fig. 2 also arises when the approximated fast implementation is used. As such, the dynamic self-organization of the particles is a robust phenomenon.

At the particle volume fractions considered here, the use of the full four-way coupling is essential for capturing large-scale dynamic clustering. This is illustrated in Fig. 3 in which we compare a structured particle field associated with four-way coupling, with a structure-less field arising in the two-way coupling model. These first impressions indicate that four-way coupling yields qualitatively different flow predictions compared to the computationally much less expensive two-way coupled description.

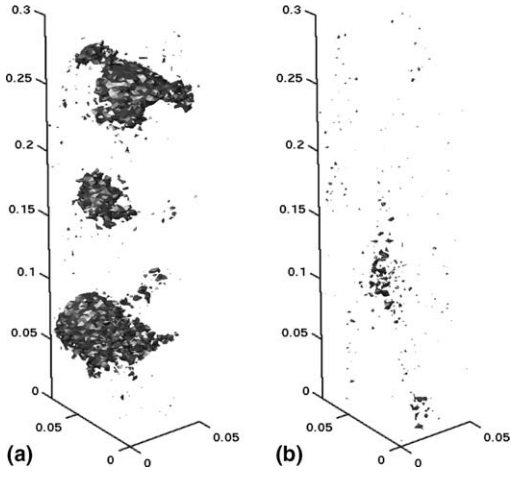

Fig. 3. Granular clustering in coherent particle-swarms is strongly associated with the four-way coupling description. Snapshot of the particle volume fraction at $t = 4$ s comparing the four-way coupling (a) with the two-way coupling (b). The iso-surfaces shown correspond to $\psi = 0.03$.

In the next section, we will quantify the effects of the gas-solids interactions by focusing on the mean gas and particle flow.

4. Turbulence modulation arising in two- and four-way coupled dynamics

In this section we will compare results obtained in 'clean' riser-flow with the particle-laden case. We will separately consider the two- and four-way coupling models. The comparison between the clean and the two-way coupling case quantifies effects due to particle–fluid and particle–wall interactions. A comparison between the two- and four-way coupled cases quantifies additional effects due to particle collisions. First, we sketch results of clean riser-flow and turn to the particle-laden case afterwards.

Clean channel. The reference 'clean' riser-flow corresponds to $Re_\tau = 180$ which coincides with the case originally reported in Moin and Kim (1982). The results for the mean streamwise fluid velocity $\langle u_z \rangle$ display only a limited variation with the adopted subgrid model as shown in Fig. 4. A close agreement with the corresponding DNS results is observed. A more sensitive assessment of the quality of LES predictions is obtained by considering rms-fluctuation levels. These also showed limited dependence on the adopted subgrid model. Compared to the unfiltered DNS data the large-eddy results yield a slight over-prediction of the fluctuation levels. This was also observed in Kuerten and Vreman (2005). In addition, the observed over-prediction of the fluctuations contains some effects of discretization errors that remain in these simulations (Geurts and Fröhlich, 2002; Meyers et al., 2003; Meyers et al., 2005).

Although the large-eddy simulations are not fully grid-independent, the grid is sufficiently fine to have a well-resolved LES of channel flow at $Re_\tau = 180$, according to the proposed criteria in Piomelli and Balaras (2002). The remaining uncertainties are small enough to allow a clear separate identification of the effects of the solids-phase on the flow-dynamics. Hence, for the purpose of assessing the dynamic effects of two- and four-way coupled discrete particles in a turbulent channel flow the adopted spatial resolution is sufficient.

Mean gas-velocity in particulate flow. We next turn to predictions of mean fluid properties for the full particle-laden flow. In Fig. 4 we collected the mean streamwise fluid velocity for the two- and four-way coupled models which display a clear turbulence modulation arising from the discrete particles. Relative to the clean channel we observe that both particle-descriptions give rise to a strongly reduced boundary layer thickness which is associated with a larger skin-friction coefficient. Consequently, Re_τ increases from 180 to 300. This puts a stronger emphasis

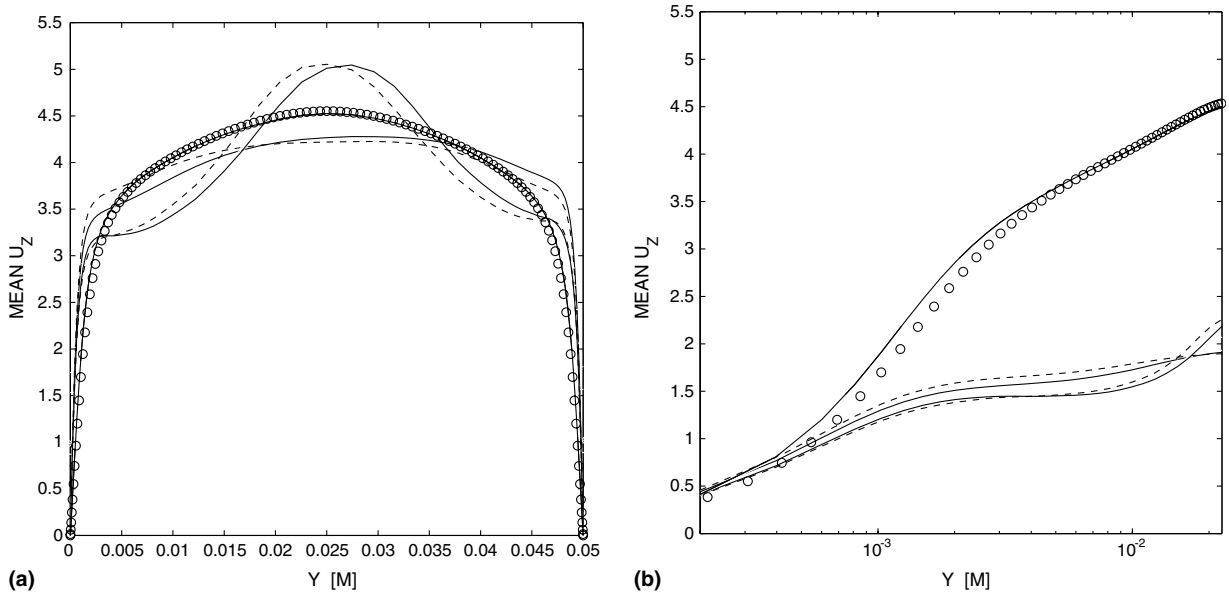

Fig. 4. Mean streamwise fluid velocity $\langle u_z \rangle$: linear (a) and logarithmic (b), comparing clean channel flow with two- and four-way coupled gas-solids flow and using different subgrid models. Standard dynamic model results (solid), approximated fast dynamic (dashed), reference DNS results of clean flow are indicated by (○). Results obtained with two-way coupling display a strong velocity-peak in the center of the channel in (a), while in (b) two-way coupling yields the lower two curves. Curves near the ○ markers correspond to the clean channel LES; the remaining curves reflect the four-way coupling.

on the accuracy of the subgrid modeling in particle-laden flow. Variations in the LES-predictions due to changes in the subgrid model hence become more pronounced in the particle-laden case.

The prediction of the bulk flow away from the boundary layers is quite different when the two-way and four-way approaches are compared. The two-way description is seen to give rise to a somewhat localized 'center-channel-jet' in which the fluid velocity is up to about 60% larger than the velocity at the edge of the boundary layer. Such a region of significantly higher velocity was not observed in the physical experiments reported in (Tsuji et al., 1984). In fact, if coarse particles at considerable volume fraction and mass load are included, the velocity profile was found experimentally to develop a flatter pattern. The results obtained using the four-way coupled description are quite in line with these earlier experimental findings.

The effects of the embedded particles on the developing flow are also reflected by the slope of the profile in the logarithmic region. Compared to the clean case an approximately logarithmic velocity profile develops for $10^{-3} < x_2 < 10^{-2}$, i.e., corresponding to $20 < y^+ < 200$, but at an increased Von Kármán 'constant'. The different LES predictions are seen to agree very well among each other; the dynamic effect of including the particles clearly dominates over variations due to changes in the subgrid model.

Mean particle properties. The consequences of particle–particle interactions for mean particle-properties are shown in Fig. 5. The strong center-jet in $\langle u_z \rangle$ observed in the two-way coupling model, is also clearly expressed in $\langle v_z \rangle$. The sensitivity of the results with respect to the adopted LES model is quite modest. The particle volume fraction distribution is shown in Fig. 5(b). A characteristic turbophoresis effect is visible in terms of an approximately 15% higher concentration near the solid walls. This effect is well established experimentally.

The factor by which the particle concentration near the wall is increased, relative to the average bulk-value, depends strongly on the precise flow-regime that is considered. Although a direct comparison with physical experiments faces important difficulties in view of differences in flow-conditions, volume fractions and particle properties, an interesting analogy with the simulation findings may be appreciated, to which we turn next.

A strong turbophoresis effect was reported by Kulick et al. (1994) for small particles at low volume fraction. Moreover, it appeared that this effect is mitigated in case particle–particle interactions can contribute more significantly to the dynamics, e.g., if the same number but larger particles was used. A similar trend was found in the simulations. In fact, the four-way coupled case studied in this manuscript displays only a modest turbophoresis effect. This limitation of the turbophoresis effect can be attributed to the fact that the particles are coarse and slowly responsive to changes in the flow. To verify this, we performed a four-way coupled simulation with particles with a much smaller diameter ($d_p = 0.04$ mm) and, consequently, a lower particle concentration ($\psi = 1.3 \times 10^{-5}$). In that case a much stronger turbophoresis was obtained in the simulation; the particle concentration near the walls increased with a factor of 30 relative to the mean bulk-concentration. This is generally consistent with the experimental work of Kulick et al. (1994) mentioned above. When two-way coupling is used in combination with coarse, slowly responsive

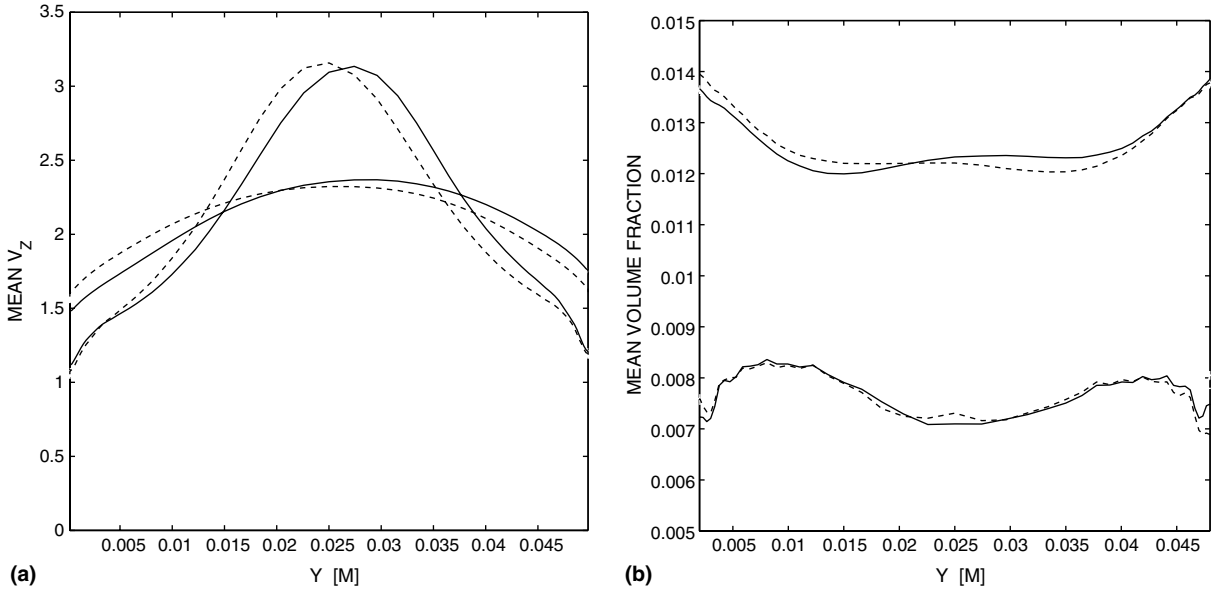

Fig. 5. Mean streamwise particle velocity $\langle v_z \rangle$ (a) and particle volume fraction $\langle \psi \rangle$ (b). Results obtained with the standard (solid) and the approximated fast (dashed) dynamic models are shown. Two-way coupled results display a velocity-peak in (a). Notice that $\langle \psi \rangle$ is shifted downward by 0.005 in (b) for the two-way results for clarity.

particles, no appreciable turbophoresis remains as is seen in Fig. 5(b). This may also be attributed to the fact that particles with much larger Stokes response-time and much larger diameter were studied, compared to (Kulick et al., 1994).

The striking differences between the resulting dynamics in the two-way and the four-way coupled descriptions of the solids-phase are directly related to the inelastic collisions which are unique to the four-way coupling. These collisions induce a spatially distributed loss of kinetic energy associated with the various particle encounters. This becomes dynamically important at sufficiently high volume fraction. As may be inferred from the results shown in Figs. 4 and 5, this additional 'dissipation' has the effect of flattening the mean streamwise velocity profiles of both the gas- and solids phase. No separate 'center-channel-jet' is observed in the four-way coupled model, in contrast to the two-way coupled description. The inelastic collisions induce the general tendency to lead to 'clustering' in the solids phase. This clustering is counteracted by the dispersive nature of the turbulent channel flow and, combined, gives rise to a complex dynamical behavior in the gas-solids flow.

5. Concluding remarks

In this paper, we presented large-eddy simulation results of particle-laden turbulent flow in a vertical riser. This flow is relevant, e.g., to chemical processing and an understanding of the fundamental dynamics of this flow is essential in order to properly predict up-scaling of processes from a laboratory scale to settings which are of industrial importance.

We showed that already at a modest particle volume fraction of about 1.5% the inelastic particle–particle interactions play an important role in the development of the flow. This is consistent with the generally accepted classification in which volume fractions larger than 10^{-3} necessitate the inclusion of particle–particle collisions (Elghobashi and Truesdell, 1993). The computationally more accessible two-way coupling model proved to give rise to qualitatively unphysical predictions, among others the occurrence of a fairly strong 'center-channel-jet' which was not recorded in experimental studies (Tsuji et al., 1984).

The presence of a large number of interacting particles leads to a strong modulation of the turbulence in the channel. Relative to a clean channel the coupling between particles and fluid is mainly responsible for the reduction in the thickness of the boundary layer and the corresponding strong increase in the skin-friction. Moreover, the log-layer that is characteristic of wall-bounded flows was seen to be retained in the particle-laden case but with an increased Von Kármán 'constant'. In addition, the particle–particle interactions in the form of inelastic collisions are mainly responsible for the flattening of the mean particle and fluid velocity distributions. These interactions also gave rise to the occurrence of dynamic self-organization of the embedded particles in coherent swarms.

Instantaneous snapshots are certainly not sufficient to describe fully the dynamic self-organization of the solids-phase. Instead, quantitative statistics need to be collected, e.g., to reveal possible characteristic time-scales associated with the clustering and dispersion. Moreover, turbulence kinetic energy budgets can provide quantitative insight into the flow physics associated with two- and four-way coupling. This will be considered in the future in combination

with a parameter-study in which central solids-phase parameters such as Stokes response-time, volume fraction and mass-load will be varied.

Acknowledgements

The authors gratefully acknowledge the use of the discrete particle software-module as developed by Kuipers, Hoomans, Goldschmidt, Link, Bokkers and Deen of the Fundamentals of Chemical Reaction Engineering Group of the University of Twente. The illustrations in Fig. 1 were kindly provided by the Physics of Fluids Group, University of Twente. Bert Vreman is grateful to the Turbulence Program of the Dutch foundation for fundamental research of matter (FOM), and to the Institute for Mechanics, Process-engineering and Control Twente (IMPACT), for financial support.

References

Bagchi, P., Balachandar, S., 2003. Effect of turbulence on the drag and lift of a particle. Phys. Fluids 15, 3496–3513.

Breugem, W.P., Boersma, B.J., 2005. Direct numerical simulations of turbulent flow over a permeable wall using a direct and a continuum approach. Phys. Fluids, 17.

Breugem, W.P., Rees, D.A.S., 2006. A derivation of the volume-averaged Boussinesq equations for flow in porous media with viscous dissipation. Transport Porous Med. 63, 1–12.

Elghobashi, S., Truesdell, G.C., 1993. On the two-way interaction between homogeneous turbulence and dispersed solid particles. I: Turbulence modification. Phys. Fluids A 5, 1790–1801.

Germano, M., Piomelli, U., Moin, P., Cabot, W.H., 1991. A dynamic subgrid-scale model. Phys. Fluids A 3, 1760–1765.

Geurts, B.J., Fröhlich, J., 2002. A framework for predicting accuracy limitations in large-eddy simulation. Phys. Fluids 14, L41–L44.

Geurts, B.J., 2003. Elements of Direct and Large-Eddy Simulation. Edwards Inc..

Hoomans, B.P.B., Kuipers, J.A.M., Briels, W.J., van Swaaij, W.P.M., 1996. Discrete particle simulation of bubble and slug formation in a two-dimensional gas-fluidized bed: a hard-sphere approach. Chem. Eng. Sci. 51, 99–118.

Kuerten, J.G.M., Vreman, A.W., 2005. Can turbophoresis be predicted by large-eddy simulation? Phys. Fluids 17, 011701.

Kulick, J.D., Fessler, J.R., Eaton, J.K., 1994. Particle response and turbulence modification in fully developed channel flow. J. Fluid Mech. 277, 109–134.

Lakehal, D., Smith, B.L., Milelli, M., 2002. Large-eddy simulation of bubbly turbulent shear flows. J. Turbulence 3, 25.

Lohse, D., Bergmann, R.P.H.M., Mikkelsen, R., Zeilstra, C., Meer, R.M., van der Versluis, M., Weele, J.P., Hoef, M.A., van der Kuipers, J.A.M., 2004. Impact on soft sand: void collapse and jet formation. Phys. Rev. Lett. 93, 198003-1–198003-4.

Marchioli, C., Giusti, A., Salvetti, M.V., Soldati, A., 2003. Direct numerical simulation of particle wall transfer and deposition in upward turbulent pipe flow. Int. J. Multiphase Flow 29, 1017–1038.

Maxey, M.R., Riley, J., 1983. Equation of motion for a small rigid sphere in a turbulent fluid flow. Phys. Fluids 26, 883.

Meyers, J., Geurts, B.J., Baelmans, M., 2003. Database-analysis of errors in large-eddy simulations. Phys. Fluids 15, 2740.

Meyers, J., Geurts, B.J., Baelmans, M., 2005. Optimality of the dynamic procedure for large-eddy simulation. Phys. Fluids 17, 045108.

Moin, P., Kim, J., 1982. Numerical investigation of turbulent channel flow. J. Fluid Mech. 118, 341.

Piomelli, U., Balaras, E., 2002. Wall-layer models for large-eddy simulations. Ann. Rev. Fluid Mech. 34, 349.

Rensen, J., Luther, S., Lohse, D., 2005. The effect of bubbles on developed turbulence. J. Fluid Mech. 538, 153–187.

Squires, K.D., Simonin, O., 2002. Recent advances and perspective of DNS and LES for dispersed two-phase flow. in: Proceedings of the 10th Workshop on Two-Phase Flow Predictions, Merseburg, pp. 152–163.

Tsuji, Y., Morikawa, Y., Shiomi, H., 1984. LDV measurements of an air-solid two-phase flow in a vertical pipe. J. Fluid Mech. 139, 417–434.

Vreman, A.W., Geurts, B.J., Deen, N.G., Kuipers, J.A.M., 2004. Large-eddy simulation of a particle-laden turbulent channel flow. In: Friedrich, R., Geurts, B.J., Metais, O. (Eds.), Direct and Large-Eddy Simulation V. Kluwer, Dordrecht, pp. 271–278.

Vreman, A.W., 2004. An eddy-viscosity model for turbulent shear-flow: algebraic theory and applications. Phys. Fluids 16, 3670–3681.

Whitaker, S., 1996. The Forchheimer equation: a theoretical development. Transport in porous media 25, 27–61.

Yamamoto, Y., Potthoff, M., Tanaka, T., Kajishima, T., Tsuji, Y., 2001. Large-eddy simulation of turbulent gas-particle flow in a vertical channel: effect of considering inter-particle collisions. J. Fluid Mech. 442, 303–334.

Zhang, D.Z., Prosperetti, A., 1997. Momentum and energy equations for disperse two-phase flows and their closure for dilute suspensions. Int. J. Multiphase Flow 23, 425–453.